

A distance estimate based on angular expansion for the planetary nebula NGC 6881

Lizette Guzmán-Ramírez,^{1*} Yolanda Gómez,² Laurent Loinard,² Daniel Tafoya³

¹*Jodrell Bank Centre for Astrophysics, University of Manchester, Manchester M13 9PL, UK*

²*Centro de Radioastronomía y Astrofísica, Universidad Nacional Autónoma de México, 58089 Morelia, Michoacán, México*

³*Department of Physics and Astronomy, Graduate School of Science and Engineering, Kagoshima University, 1-21-35 Korimoto, Kagoshima 890-0065, Japan*

Released 2011 XXXX XX

ABSTRACT

In this paper, we report on high angular resolution radio observations of the planetary nebula NGC 6881 obtained with the Very Large Array at a wavelength of 6 cm. The emission appears to be the superposition of a roundish core and a point-symmetric bipolar structure elongated along a position angle of about 145° . This is strongly reminiscent of the morphology seen in $H\alpha$ and [NII] images. A comparison between VLA observations obtained in 1984 and 1994 clearly reveals the expansion of the core of the nebula, at a rate of $2.1 \pm 0.7 \text{ mas yr}^{-1}$. Assuming that the expansion velocity in the plane of the sky (determined from these measurements) and the expansion velocity along the line of sight (estimated from optical spectroscopy available in the literature) are equal, we find a distance to NGC 6881 of $1.6 \pm 0.5 \text{ kpc}$. This distance is compatible with (but does not necessarily imply) an association of NGC 6881 with the nearby HII region Sh 2-109 and, more generally, the Cygnus star-forming region.

Key words: planetary nebulae: general — planetary nebulae: individual (NGC 6881, PG 74.5+02.1) — astrometry — stars: late type

1 INTRODUCTION

NGC 6881 (PG 74.5+02.1, IRAS 20090+3715) is a very interesting planetary nebula (PN) with a system of multiple bipolar lobes traced by the emission from ionized as well as neutral material (Guerrero & Manchado 1998; Guerrero et al. 2000; Kwok & Su 2005; Ramos-Larios et al. 2008). Originally, Guerrero & Manchado (1998) classified it as a quadrupolar planetary nebula based on the examination of the [N II] emission and the [N II]/[O III] and [N II]/ $H\alpha$ ratio images. These authors found one pair of lobes consisting of two highly collimated structures that finish as bright knots where the emission of [NII] is enhanced (outer lobes). With a size of about $8''$, the inner lobes are shorter but much brighter than their outer counterparts. Moreover, they exhibit a clear point-symmetric morphology. The expansion velocity derived for these lobes is 90 km s^{-1} , which yields a kinematical age of about $400d$ years (where d is the source distance in kpc).

Kwok & Su (2005) obtained Hubble Space Telescope images of this nebula from which they identified one more pair of ionized lobes. They have the same extension and morphology as the inner lobes but with a position angle slightly different. This discrepancy is not well understood. These authors also found several rings circumscribed in the inner walls of the ionized bipolar lobes. The presence of these multipolar lobes and rings oriented in different directions suggests the action of precessing collimated fast

outflows that change their precession axis as a function of time. Guerrero & Manchado (1998) proposed this to explain the existence of a loop-like structure traced by the ionized emission, located at the southeast edge of the lobes and elongated in the direction perpendicular to the lobes. They modeled the loop as a precessing jet that, assuming ballistic expansion, started $\sim 7400d$ years ago. However, Ramos-Larios et al. (2008) found that the location of the loop-like structure coincides perfectly with the ending tip of the southeast H_2 lobe, suggesting that it is marking a region of interaction of the bipolar lobe with dense material. These authors noted that NGC 6881 is projected towards the HII region Sh 2-109 and suggested that they are physically associated. They proposed that the southeast lobe of NGC 6881 is interacting with dense material, forming the observed loop-like structure and the sharp edge of the H_2 lobe. The HII region Sh 2-109 is located at a distance of $1.4 \pm 0.4 \text{ kpc}$ (Fich & Blitz 1984). Using a distance scale proposed by Cahn et al. (1992), Ramos-Larios et al. (2008) calculated a distance of $\sim 1.5 \text{ kpc}$ to NGC 6881, which supports the association with the region Sh 2-109. However, the scale developed by Zhang (1995) yields a distance of 6.4 kpc , in which case they would not be physically associated.

Statistical techniques can provide distance estimates to PNe as accurate as 50% on average, but when they are applied to individual objects the errors can be as large as a factor of 2 or even more (e.g. Tafoya et al. 2011). This results in a very uncertain estimation of the Galactic location and physical parameters of PNe. In order to obtain more accurate estimations of the

* lizette.ramirez@postgrad.manchester.ac.uk

Table 1. Observational parameters

Epoch	Phase Calibrator	Bootstrapped Flux density
1984 Dec 29 (1984.99)	2023+336	2.07±0.01 Jy
1994 Mar 31 (1994.24)	2005+403	2.98±0.01 Jy

distance to PNe, other techniques have been used. One that has proven effective is the so-called expansion parallax method, which is based on the comparison of the angular expansion of the source on the plane of the sky, with the velocity expansion along the line of sight measured from the width of some appropriately chosen spectral lines (Masson 1986). In principle, the angular expansion could be measured using any tracer, but the free-free radio emission from the ionized gas has been, by far, the most popular choice (Masson 1986, 1989; Gómez et al. 1993; Hajian et al. 1993, 1995; Kawamura & Masson 1996; Hajian & Terzian 1996; Christianto & Seaquist 1998; Guzmán et al. 2006; Zijlstra et al. 2008; Guzmán et al. 2009). Hubble Space Telescope observations at optical wavelengths have also occasionally been used to measure the expansion (Reed et al. 1999; Palen et al. 2002).

In this work we have used the expansion parallax method to measure the distance to the PN NGC 6881. Our new distance estimate will be used to determine with improved accuracy the physical parameters of the source, particularly its size and age. It will also enable us to examine the association of NGC 6881 with the HII region Sh 2-109. For this purpose, we have retrieved data from the Very Large Array (VLA) archive of the National Radio Astronomy Observatory¹ (§2). The structure of NGC 6881 and the details of the component that was used for the measurements are described in §3. The technique used to determine the angular expansion is presented in §4. The estimation of the distance and the location of NGC 6881 in our Galaxy, as well as other physical parameters, are discussed in §4.1.

2 THE DATA

We have made use of two data sets of observations toward the PN NGC 6881 retrieved from the VLA archive. The observations were performed in the continuum mode (bandwidth = 50 MHz) at a frequency of 4.8 GHz (corresponding to a wavelength of 6 cm). The configuration of the array for both data sets was the most extended one (configuration A). The two data sets correspond to observations carried out on 1984, December 29 (1984.99; project AK113) and 1994, March 31 (1994.24; project AH509), respectively. This gives a time baseline of 9.25 years between the observations. The data were edited and calibrated using the Astronomical Image Processing System (AIPS) following standard procedures (see Table 1). Both data sets were self-calibrated in phase and amplitude.

3 THE STRUCTURE OF THE PN NGC 6881

In the radio continuum images, NGC 6881 clearly exhibits a bipolar, point-symmetric structure elongated along a position angle of 145° (see Fig. 1). This morphology is very similar to that of the H α , [NII] and [OIII] images presented by Guerrero & Manchado

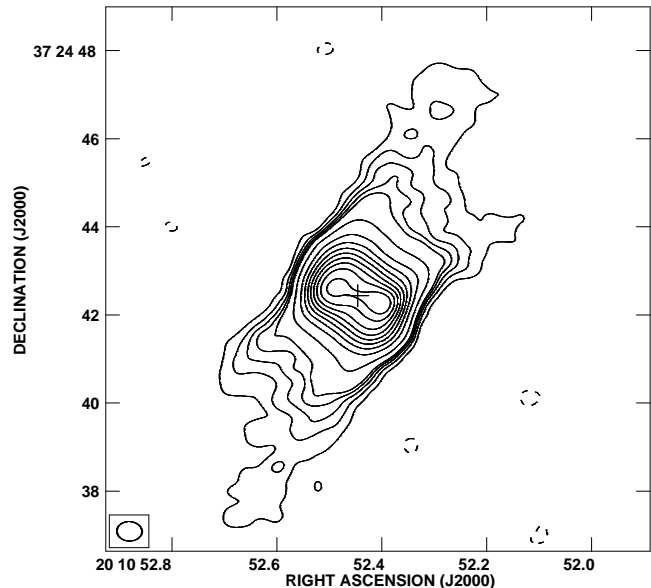


Figure 1. Contour image of the 4.8 GHz (6 cm) continuum emission from NGC 6881 for the 1994.24 epoch. The contours are -1, 1, 2, 3, 4, 5, 10, 20, 30, 40, 50, 60, 70, 80, and 90% the peak flux of 9.8 mJy beam⁻¹. The *rms* noise of the image is 0.025 mJy beam⁻¹. The synthesized beam (0''.57 × 0''.44 with a position angle of 87°) is shown in the bottom left corner of the image. The cross marks the position adopted as the center of the nebular emission: $\alpha(2000) = 20^h 10^m 52^s.446$, $\delta(2000) = +37^\circ 24' 42''.43$.

(1998), although the radio continuum emission image is not as sensitive in the outermost portions of the lobes as those in H α and [NII]. In consequence, neither the knots nor the loop-like structure, which are detected in [NII] light, are detected in radio continuum emission. In the central region of the nebula, a two-peaked bright core (also seen in [NII] images) elongated along a position angle of 55° is clearly present. Guerrero & Manchado (1998) interpreted this structure as an expanding ring in the equatorial plane of the nebula.

If we assume that the expansion velocity of the central core along the line of sight is the same as that on the plane of the sky, the angular expansion rate should be about 2 mas yr⁻¹ if the source is at 1.5 kpc and about 0.5 mas yr⁻¹ for $d = 6.4$ kpc. Such values, although small, are measurable, provided the core of the emission can be separated from the lobes. For interferometric data, the structures associated with different angular scales can be separated by restricting the portion of the ($u - v$) plane considered during the imaging process (Gómez et al. 1993). In the case of NGC 6881 the emission from the extended lobes can be almost entirely suppressed by selecting only the visibilities corresponding to ($u - v$) spacings longer than about 30 k λ (corresponding to $\sim 7''$). In addition, the expansion is best detected if the longest ($u - v$) spacings are somewhat down-weighted and the angular resolution is degraded so the source is only a few resolution elements across (e.g. Gómez et al. 1993). In the present case, this was achieved by considering only visibilities in the ($u - v$) range from 30 to 550 k λ , and by applying a Gaussian taper function with a full width at half maximum of 200 k λ . Finally, the images were reconstructed to minimize possible differences in the $u - v$ coverage using a beam of 0''.87 × 0''.80, P.A. = 0°, the average of the individual beams of each observation. These procedures yielded noise levels of ~ 0.09 and 0.05 mJy beam⁻¹, for the 1984 and 1994 data sets, respectively. The difference image between the two epochs (1994.24–1984.99), was produced following Guzmán

¹ The NRAO is operated by Associated Universities, Inc. under a cooperative agreement with the National Science Foundation.

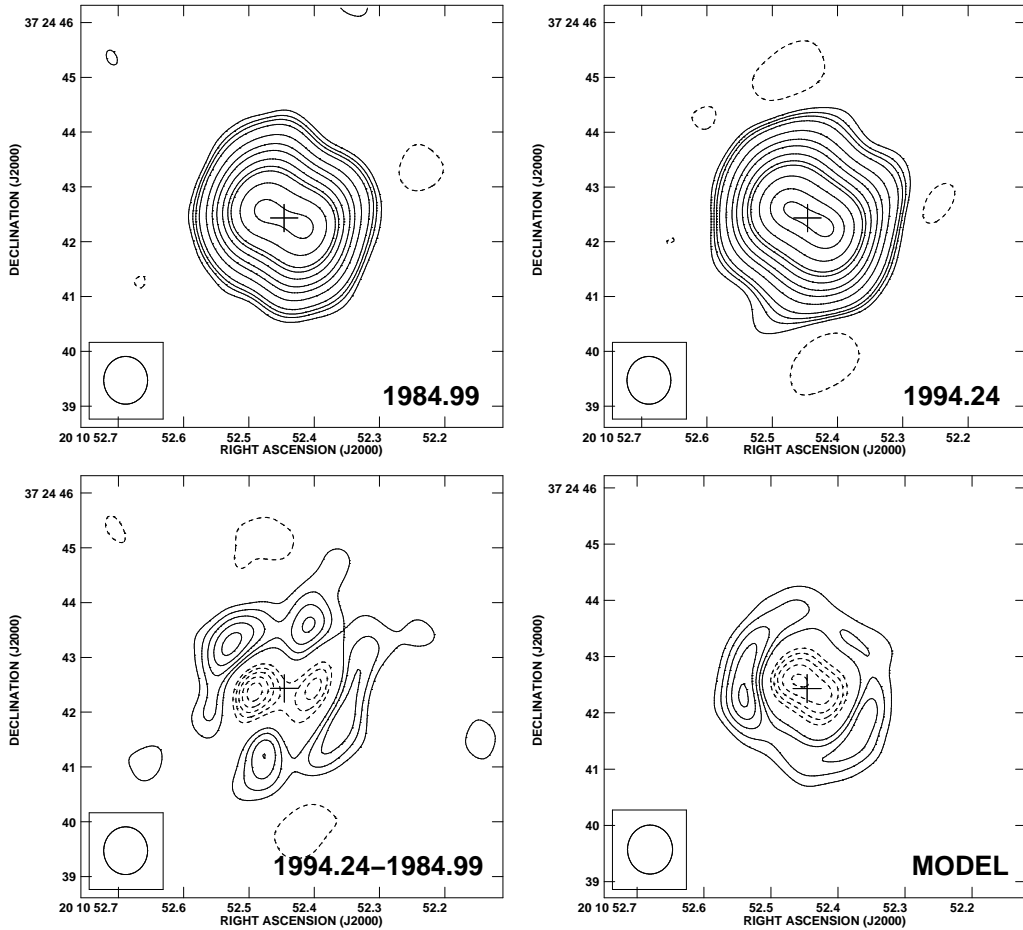


Figure 2. Top: Reconstructed contour images of the 6 cm continuum emission from NGC 6881 for 1984.99 (left) and 1994.24 (right). The contours are $-4, 4, 7, 10, 15, 30, 50, 70, 100, 130, 150, 200, 250$, and 280 times $0.07 \text{ mJy beam}^{-1}$, the average *rms* noise of the images. The individual *rms* of the images is $0.09 \text{ mJy beam}^{-1}$ for the 1984.99 image and $0.05 \text{ mJy beam}^{-1}$ for the 1994.24 image. Bottom: contour images of the 6 cm difference image (left) and of the best model (right) obtained as described in the text. The contours are $-11, -9, -7, -5, -3, 3, 5, 7, 9$, and 11 times $0.095 \text{ mJy beam}^{-1}$, the *rms* noise of the difference image. The restoring beam ($0''.87 \times 0''.80$ with a position angle of 0°) is shown in the bottom left corner of each image.

et al. (2006, 2009), and is shown in the bottom left panel of Figure 2. This image shows the typical negative and positive pattern expected when expansion is present.

4 ESTIMATION OF THE ANGULAR EXPANSION

The images of NGC 6881 obtained at epochs 1984.99 and 1994.24 (upper panels of Figure 2) look very similar, so the expansion of the nebula is not immediately obvious. The negative-positive pattern seen in the difference image (1994.24–1984.99), however, clearly reveals the expansion of the ionized nebula. Gómez et al. (1993), and more recently Guzmán et al. (2006, 2009) have developed a technique that has proven effective to measure very small expansion rates using observations at two epochs. The technique is based on the assumption that the expansion of the ionized nebula is self-similar. To characterize the expansion, the image corresponding to the better of the two data sets is self-similarly expanded by a factor $1 + \epsilon$ (if the best data set corresponds to the older observation) or shrunk by a factor $1 - \epsilon$ (if it is the more recent), and subtracted from itself. This provides a model difference image that can be compared with the true difference image. The correct expansion rate clearly corresponds to the value of ϵ for which the model difference image

is most similar to the measured difference image. Quantitatively, this corresponds to the value of ϵ that minimizes the χ^2 defined as

$$\chi^2 = \sum_{i,j} (M_{i,j} - T_{i,j})^2 / \sigma^2, \quad (1)$$

where $M_{i,j}$ is the value at pixel (i, j) in the model difference image, $T_{i,j}$ is the value at the corresponding pixel of the true difference image and σ is the standard deviation of the data. The sum is taken over the appropriate portion of the images.

In the present case, the data obtained at epoch 1994.24 have better quality, so the corresponding image was contracted by a factor $(1 - \epsilon)$. The value of the χ^2 as a function of ϵ is shown in Figure 3. It has a clear minimum at $\epsilon = 0.027$. The model difference image corresponding to that value of ϵ is shown in the bottom right panel of Figure 2. Once the minimum value of ϵ is determined, the confidence limits on this value are estimated as follows. The number of independent data points in the fit, n , is estimated by dividing the solid angle of the region used to estimate ϵ by the solid angle of the synthesized beam. Here, the region of the images considered to calculate the χ^2 corresponds to $n = 20$ beams. Assuming that the plot in Figure 3 represents a normal χ^2 distribution and following Press et al. (1992), we scale by multiplication the value of the minimum to be 20. The confidence limits are estimated by determining

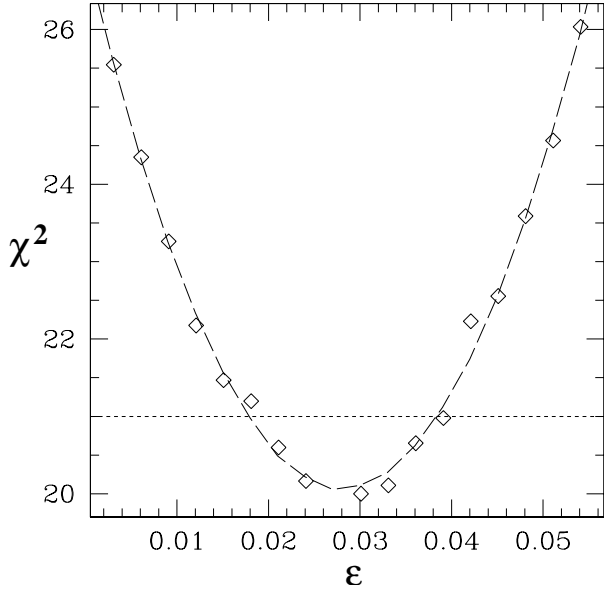


Figure 3. χ^2 fit of the residual image obtained from subtracting the model to the data as function of the contraction factor ϵ . The minimum of the fitted curve (dashed-line) indicates the value of ϵ that minimizes the χ^2 function.

Table 2. Observational parameters

Epoch	Phase Calibrator	Bootstrapped Flux density
1984 Dec 29 (1984.99)	2023+336	2.07 ± 0.01 Jy
1994 Mar 31 (1994.24)	2005+403	2.98 ± 0.01 Jy

the ϵ interval given for a value in the horizontal axis of $n + 1 = 21$ (Avni 1976; Wall 1996). This yields $\epsilon = 0.027 \pm 0.010$.

The good agreement between the images produced for the real difference and the model difference suggests that the assumption of self-similar expansion for the central ring of the PN NGC 6881 is reasonable, at least in the equatorial plane of the nebula. The structure in the direction of the bipolar lobes appears to be more complex, and a different expansion velocity (~ 90 km s⁻¹; Guerrero & Manchado 1989) might be more appropriate. Moreover, as we mentioned earlier, the outflow direction may be changing with time (Kwok & Su 2005). Therefore, a 2D or 3D model (such as that presented by Zijlstra et al. (2008) for NGC 7027) would, in principle, be needed. However, constructing a detailed kinematic model of NGC 6881 would require unavailable additional observations and, at any rate, the value of ϵ found here is almost entirely constrained by the expansion of the central core/ring. Thus, as long as we restrict ourselves to this specific component, our determination provides an accurate estimate of the expansion. From the value of ϵ estimated earlier, the angular expansion rate of NGC 6881 can be calculated as:

$$\dot{\theta} = \frac{\theta \epsilon}{\Delta t}, \quad (2)$$

where, θ is the radius of the ring and Δt is the time baseline between the observations. From the separation of the two peaks seen in the full free-free emission images (Figure 1), we estimate that the radius of the ring is $0''.73 \pm 0''.01$, and an angular expansion rate of $\dot{\theta} = 2.1 \pm 0.7$ mas yr⁻¹ for the central ring of NGC 6881.

4.1 The distance to NGC 6881

The distance d to NGC 6881 can be obtained from its angular expansion rate as:

$$\left[\frac{d}{\text{pc}} \right] = 211 \left[\frac{v_{\text{exp}}}{\text{km s}^{-1}} \right] \left[\frac{\dot{\theta}}{\text{mas yr}^{-1}} \right]^{-1}, \quad (3)$$

where v_{exp} is the expansion velocity of the central ring along the line of sight. As mentioned previously, the expansion velocity of the ring has been estimated from the line splitting of the [NII] by Guerrero & Manchado (1998) to be $v_{\text{exp}} = 14.0$ km s⁻¹. Other estimates of the expansion velocity of NGC 6881 using [OIII] lines resulted in values of 18 km s⁻¹ (Robinson et al. 1982) and 16.5 km s⁻¹ (Weinberger 1989). Thus, we will use an average expansion velocity value of $v_{\text{exp}} = 16 \pm 2$ km s⁻¹. This leads to a distance $d = 1.6 \pm 0.5$ kpc; table 2 shows the physical parameters of NGC 6881 calculated using this value.

The distance found here is in good agreement with that obtained by Ramos-Larios et al. (2008), $d \sim 1.5$ kpc. It is also compatible with the physical association of NGC 6881 with the nearby HII region Sh 2-109 (see §1). When superimposed over the extended HI emission (Cappa et al. 1996), NGC 6881 appears projected toward a cavity with a $v_{\text{LSR}} \sim 10$ km s⁻¹, very close to that of the Cyg OB1 association. The estimated distance to this association lies in the range 1.25–1.83 kpc (Lozinskaya et al. 1998; Schneider et al. 2006). The association Cyg OB 1 is located to the south-west of the Cygnus star-forming region. Recently, Rygl et al. (2010) measured very accurately the parallax of the massive star-forming region W75N with the Cygnus region and found $d = 1.32^{+0.11}_{-0.09}$ kpc. This suggests that the entire Cygnus complex (which is about 200 pc across) is located to distances between 1.2 and 1.8 pc. Thus, our result supports the idea that NGC 6881 might be associated with the massive star forming region in Cygnus. Although this may be a simple coincidence, it may also indicate that the progenitor of NGC 6881 could have been a short-lived intermediate-mass star. Interestingly, some of the observed characteristics of NGC 6881 may be readily interpreted in this scheme. Ramos-Larios et al. (2008) observed that the southeast H2 lobe of NGC 6881 is less extended than its northwest counterpart, and shows a sharp edge. They note that a possible explanation for this asymmetry would be an interaction between the lobes of NGC 6881 and inhomogeneous interstellar gas. This could occur naturally if NGC 6881 were indeed associated with the star-forming region.

5 CONCLUSIONS

We have presented observations of the planetary nebulae NGC 6881 obtained using the VLA at 6 cm (4.8 GHz) at two epochs separated by 9.25 years. Assuming a self-similar expansion for the ionized gas, we determine an expansion angular rate for NGC 6881 of 2.1 ± 0.7 mas year⁻¹, and a distance of 1.6 ± 0.5 kpc. This places NGC 6881 at the same distance as the HII region Sh 2-109 and the Cygnus star-forming region.

6 ACKNOWLEDGMENTS

L.G., Y.G. and L.L. acknowledge the support of DGAPA, UNAM and CONACYT (México). L.L. is indebted to the Guggenheim Foundation for financial support. D.T. acknowledges support from the Japan Society for Promotion of Science (project ID: 22-00022). We gratefully acknowledge useful discussions with L. F.

Rodríguez; this paper would not have been the same without his comments. We also all acknowledge the comments and help of the Referee. This research has made use of the SIMBAD database, operated at CDS, Strasbourg, France.

REFERENCES

- Avni Y., 1976, *ApJ*, 210, 642
- Cahn J. H., Kaler J. B., Stanghellini L., 1992, *A&AS*, 94, 399
- Cappa C. E., Dubner G. M., Rogers C., St-Louis N., 1996, *AJ*, 112, 1104
- Christianto H., Seaquist E. R., 1998, *AJ*, 115, 2466
- Fich M., Blitz L., 1984, *ApJ*, 279, 125
- Gómez Y., Rodríguez L. F., Moran J. M., 1993, *ApJ*, 416, 620
- Guerrero M. A., Manchado A., 1998, *ApJ*, 508, 262
- Guerrero M. A., Villaver E., Manchado A., Garcia-Lario P., Prada F., 2000, *ApJS*, 127, 125
- Guzmán L., Gómez Y., Rodríguez L. F., 2006, *Revista Mexicana de Astronomía y Astrofísica*, 42, 127
- Guzmán L., Loinard L., Gómez Y., Morisset C., 2009, *AJ*, 138, 46
- Hajian A. R., Terzian Y., 1996, *Public. of the Astron. Soc. Pac.*, 108, 419
- Hajian A. R., Terzian Y., Bignell C., 1993, *AJ*, 106, 1965
- Hajian A. R., Terzian Y., Bignell C., 1995, *AJ*, 109, 2600
- Kawamura J., Masson C., 1996, *ApJ*, 461, 282
- Kwok S., Su K. Y. L., 2005, *ApJL*, 635, L49
- Lozinskaya T. A., Pravdikova V. V., Sitnik T. G., Esipov V. F., Mel’Nikov V. V., 1998, *Astronomy Reports*, 42, 453
- Masson C. R., 1986, *ApJL*, 302, L27
- Masson C. R., 1989, *ApJ*, 336, 294
- Palen S., Balick B., Hajian A. R., Terzian Y., Bond H. E., Panagia N., 2002, *AJ*, 123, 2666
- Press W. H., Teukolsky S. A., Vetterling W. T., Flannery B. P., 1992, *Numerical recipes in FORTRAN. The art of scientific computing*
- Ramos-Larios G., Guerrero M. A., Miranda L. F., 2008, *AJ*, 135, 1441
- Reed D. S., Balick B., Hajian A. R., Klayton T. L., Giovanardi S., Casertano S., Panagia N., Terzian Y., 1999, *AJ*, 118, 2430
- Robinson G. J., Reay N. K., Atherton P. D., 1982, *MNRAS*, 199, 649
- Rygl K. L. J., Brunthaler A., Menten K. M., Reid M. J., van Langevelde H. J., Honma M., Torstensson K. J. E., Fujisawa K., Sanna A., 2010, *ArXiv e-prints*
- Schneider N., Bontemps S., Simon R., Jakob H., Motte F., Miller M., Kramer C., Stutzki J., 2006, *A&A*, 458, 855
- Tafoya D., Imai H., Gomez Y., Torrelles J. M., Patel N. A., Anglada G., Miranda L. F., Honma M., Hirota T., Miyaji T., 2011, *ArXiv e-prints*
- Wall J. V., 1996, *Quarterly Journal of the Royal Astron. Soc.*, 37, 519
- Weinberger R., 1989, *A&AS*, 78, 301
- Zhang C. Y., 1995, *ApJS*, 98, 659
- Zijlstra A. A., van Hoof P. A. M., Perley R. A., 2008, *ApJ*, 681, 1296